Partial wave analysis of $\bar{p}p$ annihilation channels in flight with $I = 1, C = +1$

A.V. Anisovich[c], C.A. Baker[b], C.J. Batty[b], D.V. Bugg[a], V.A. Nikonov[c], A.V. Sarantsev[c], V.V. Sarantsev[c], B.S. Zou[a] [1]

[a] *Queen Mary and Westfield College, London E1 4NS, UK*
[b] *Rutherford Appleton Laboratory, Chilton, Didcot OX11 0QX,UK*
[c] *St. Petersburg Nuclear Physics Institute, Gatchina, St. Petersburg district, 188350, Russia*

Abstract

A combined analysis is reported of $3\pi^0$, $\pi^0\eta$ and $\pi^0\eta'$ data in the mass range 1960 to 2410 MeV. This analysis is made consistent also with $\eta\eta\pi^0$ data, reported separately. The analysis requires s-channel resonances with a spectrum close to that published earlier for $C = +1$ states with $I = 0$; masses for $I = 1$ states are lower on average by 20 MeV. Two alternative solutions are found, differing only for $J^P = 2^+$ and 4^+ states by small amounts in masses and widths. Both $3\pi^0$ and $\eta\pi^0$ data prefer one of these two solutions. For this preferred solution, observed states have J^{PC}, masses and widths (M, Γ) in MeV as follows: 4^{-+}: $(2250\pm15, 215\pm25)$, 4^{++}: $(2255\pm40, 330^{+110}_{-50})$ and $(2005^{+25}_{-45}, 180\pm30)$, 3^{++}: $(2275 \pm 35, 350^{+100}_{-50})$ and $(2031 \pm 12, 150 \pm 18)$, 2^{-+}: $(2245 \pm 60, 320^{+100}_{-40})$ and $(2005 \pm 15, 200 \pm 40)$, 2^{++}: $(2255 \pm 20, 230 \pm 15)$, $(2175 \pm 40, 310^{+90}_{-45})$ and $(2030 \pm 20, 205 \pm 30)$, and 1^{++}: $(2270^{+55}_{-40}, 305^{+70}_{-35})$. There are indications of further 2^{-+}, 2^{++} and 1^{++} contributions just below the available mass range, and also a 0^{++} state at ~ 2025 MeV.

Data for $\bar{p}p \to 3\pi^0$ have been reported earlier [1] from the Crystal Barrel experiment at LEAR in the momentum range 600 to 1940 MeV/c. Data from channels $\bar{p}p \to \pi^0\eta$ and $\pi^0\eta'$ have also been presented [2]. There is evidence for a number of s-channel resonances with similar masses and widths in the two analyses. The objective here is to report a combined analysis with consistent resonance parameters in all three sets of data.

A related analysis of $\bar{p}p \to \eta\eta\pi^0$ in reported separately [3]. Those data provide evidence for two 0^- resonances which are less conspicuous in the $3\pi^0$ data discussed here. The present analysis uses the parameters of those resonances. Conversely, the analysis of $\eta\eta\pi^0$ uses parameters of resonances reported here. It is useful to examine the sensitivity of each set of data to individual resonances.

A second objective is to compare resonance masses and widths with a combined analysis reported earlier [4] of $I = 0$, $C = +1$ channels $\pi^0\pi^0$, $\eta\eta$, $\eta\eta'$, $\eta\pi^0\pi^0$ and $\pi^+\pi^-$. There, a complete spectrum of the $q\bar{q}$ states expected in this mass range was found, as well as some additional states. If mass differences between u and d quarks are small, as is generally believed, the spectra for $I = 1$ and 0 should be similar. This is what we find.

We outline first the considerations going into the partial wave analysis. The earlier study of $3\pi^0$ data fitted magnitudes and phases of amplitudes separately to data at individual momenta. Those results were then interpreted in terms of s-channel resonances for $J^P = 4^+$, 3^+, 2^+ and 1^+. For $\pi^0\eta$ and $\pi^0\eta'$, magnitudes and phases of $\pi^0\eta$ and $\pi^0\eta'$ amplitudes were close to SU(3)

---

[1]Now at IHEP, Beijinj 100039, China

relations [2]. The composition of η and η' are well known from a study of many branching ratios [5] to be

$$|\eta> = \cos\theta|\frac{u\bar{u} + d\bar{d}}{\sqrt{2}}> - \sin\theta|s\bar{s}> \tag{1}$$

$$|\eta'> = \sin\theta|\frac{u\bar{u} + d\bar{d}}{\sqrt{2}}> + \cos\theta|s\bar{s}>, \tag{2}$$

with $\cos\theta \simeq 0.8$ and $\sin\theta \simeq 0.6$. The same SU(3) constraints are applied here.

Partial wave amplitudes are expressed as sums of s-channel resonances plus backgrounds. Each resonance is fitted to a Breit-Wigner amplitude of constant width with real coupling constant g and phase angle ϕ:

$$f = \frac{\sqrt{\rho_{\bar{p}p}(p)}}{k} \frac{g\exp(i\phi)B(p)B(q)}{M^2 - s - iM\Gamma}. \tag{3}$$

Backgrounds are parametrised as constants or linear functions of s, or as resonances below the $\bar{p}p$ threshold. These assumptions impose the important constraint of analyticity. Blatt-Weisskopf centrifugal barrier factors B are included explicitly for coupling to $\bar{p}p$ (momentum p in the overall centre of mass frame) and coupling to the decay channel (momentum q); the radius of the centrifugal barrier is set to 0.83 fm from Ref. [4]. The factor $1/k$ allows for the flux in the $\bar{p}p$ entrance channel, and $\rho_{\bar{p}p}$ is the phase space in the $\bar{p}p$ channel.

Partial waves with $J^P = 2^+$ and 4^+ may couple to $\ell = J \pm 1$ in the $\bar{p}p$ channel, e.g. $^3F_2$ and $^3P_2$. Multiple scattering through the resonance is expected to lead to approximately the same phase ϕ for both ℓ values. For $I = 0$ $C = +1$, phases are accurately determined; all phase differences between $\ell = J \pm 1$ lie in the range $0 \pm 15°$. For present data, they are less accurately determined (because of the lack of polarisation data) but are consistent with zero. We therefore fit the ratio of coupling constants g_{J+1}/g_{J-1} to a real ratio r_J. Most states turn out to be dominantly $L = J - 1$ or $L = J + 1$, and the larger partial wave governs the determination of resonance masses and widths.

The amplitude analysis turns out to be much less secure than for $I = 0$, $C = +1$ for several reasons. The fundamental reason is that no data are available from a polarised target, as was the case for $I = 0$ in the $\pi^-\pi^+$ channel. Polarisation data play two fundamental roles. Firstly, they separate amplitudes with helicities 0 and 1 in the initial state, hence $\ell = J \pm 1$. In the present analysis, separation between $^3P_2$ and $^3F_2$ amplitudes and between $^3F_4$ and $^3H_4$ is hampered by the absence of such polarisation information. The second role of polarisation data is that they are phase sensitive. Polarisation measures the imaginary part of interferences between partial waves, while differential cross sections are sensitive to the real parts of interferences. For $I = 0$, $C = +1$, the availability of both differential cross sections and polarisations puts tight constraints on all phases. For the present $I = 1$, $C = +1$ channels, relative phases are poorly determined when the phase angle between partial waves is close to 0 or π, because of the lack of polarisation data. This leads to larger errors for several resonances.

A second problem is as follows. Dalitz plots for $3\pi^0$ data are shown at four representative momenta in Fig. 1. There is just one dominant signal, $f_2(1270)\pi$, from which to search for resonances. Underneath the $f_2(1270)$ bands is a broad physics background. This is fitted as $\sigma\pi$, where σ stands for the $\pi\pi$ S-wave amplitude as parametrised in Ref. [6]. Because of the
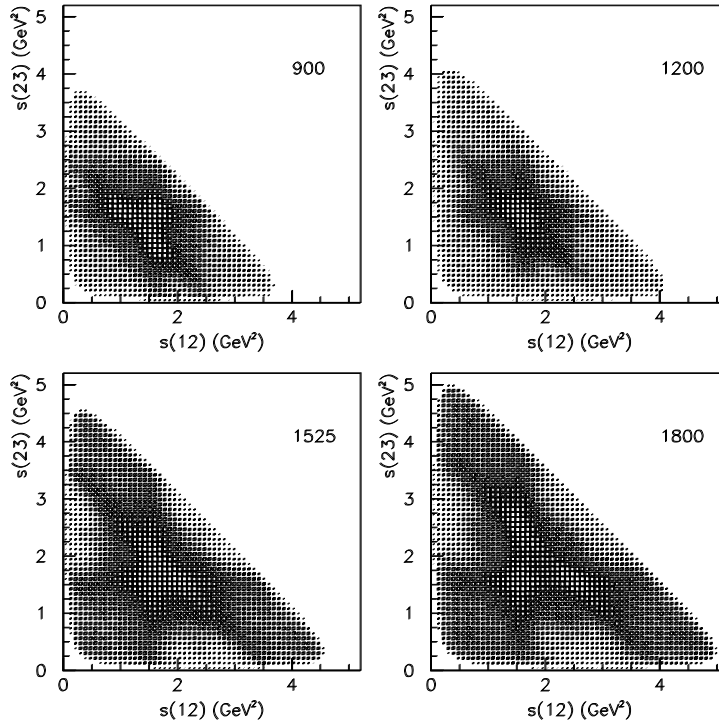
Figure 1: Dalitz plots for data; numbers in each panel indicate beam momenta in MeV/c.

sixfold symmetry of the Dalitz plot, it is hard to separate contributions from low and high masses in $\pi\pi$. The σ amplitude varies slowly with s and its coupling constant is likely to have some s-dependence. We assume the coupling constant may vary linearly with s. There must also be contributions from so-called triangle diagrams [7]. One of the pions from the decay of $f_2(1270)$ may rescatter from the spectator pion, producing a new resonance. In principle such processes are calculable. They lead to a logarithmic variation of the amplitude with s. Such processes cannot in practice be separated from the $\pi\pi$ S-wave amplitude. In summary, there is an intrinsic uncertainty about how to parametrise the background. Different parametrisations lead to somewhat different interferences with $f_2(1270)$ bands. Since the broad background appears dominantly in the $J^P = 0^-$ channel, these differences introduce uncertainties mostly into the determination of singlet partial waves with $J^P = 0^-$, 2^- and 4^-.

The fit to angular distributions in Fig. 2 at 1200 and 1350 MeV/c is not perfect. The problem is associated with the crossing of three $f_2(1270)$ bands, visible on Fig. 1. A possible explanation is that triangle effects of Ref. [7] will have maximum effect at this triple intersection.

A third problem, purely experimental, is that the production angular distribution for $f_2(1270)$ shows an extremely rapid change between the two lowest momenta, 600 and 900 MeV/c. It is illustrated in the first two panels of Fig. 2. This makes it hard to determine resonance parameters for the lower group of s-channel resonances which cluster in this range. The analysis of $I = 0$, $C = +1$ was on firmer ground, because of the availability of data for $\bar{p}p \to \pi^-\pi^+$ at 100 MeV/c steps from 360 to 900 MeV/c, both differential cross sections and polarisations; those data extend down to a mass of 1910 MeV.

A defect in our earlier analyses in Refs. [1] and [2] was that $3\pi^0$ data were fitted with only two 2^+ resonances, while those for $\pi^0\eta$ and $\pi^0\eta'$ were fitted with three. They also used different values of the ratios r_2 between $^3F_2$ and $^3P_2$ amplitudes and likewise for r_4 between $^3H_4$ and $^3F_4$. These defects are rectified here. It turns out to be quite difficult to find a combined fit
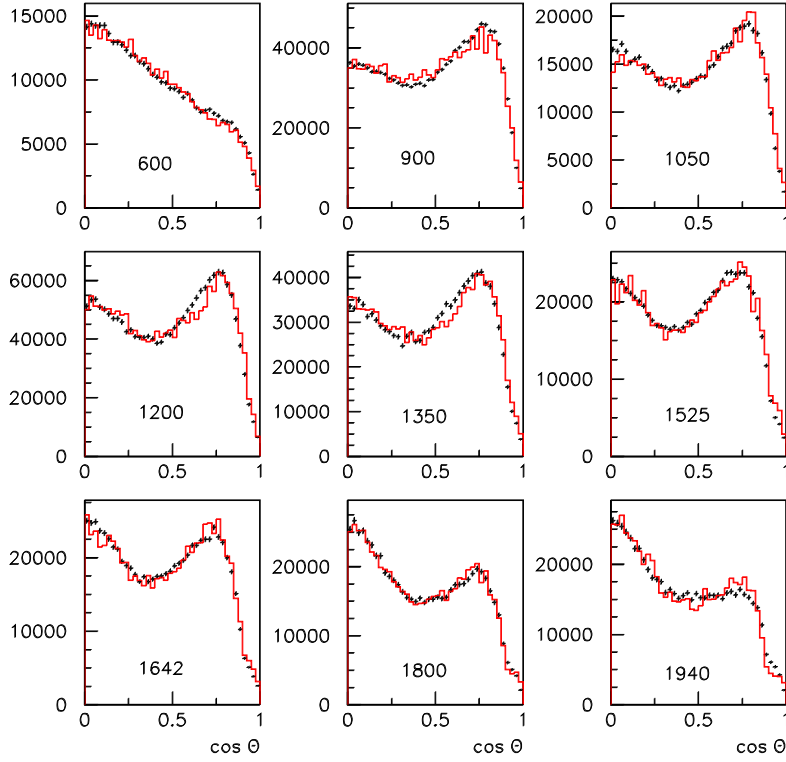
3

Figure 2: Angular distributions for production of $f_2(1270)\pi$ for events with at least one value of $M(\pi\pi)$ in the range 1175–1375 MeV. Histograms show the partial wave fit. Numbers in each panel indicate the beam momentum in MeV/c.

to all data with consistent values of r_2 and r_4. A good fit requires that r_2 varies rapidly over the available mass range. Four 2^+ states are required. This agrees with $I = 0$, $C = +1$, where two dominantly $^3P_2$ states were found at 1934 and 2210 MeV and two dominantly $^3F_2$ states at 2010 and 2293 MeV. A similar pattern emerges here. As a result, fits to data have changed significantly from the earlier publications for partial waves with $J^P = 2^+$ and 4^+.

This change is particularly large for $3\pi^0$ data at the lowest two momenta. The fit shown in Ref. [1] had a large $^3P_1$ intensity there. However, we now find that adding further $^3P_2$ states at ~ 1950 and 2175 MeV produces a very large improvement in the fit, by ~ 10500 in log likelihood. There is large cross-talk at low momenta between $^3P_2$ and $^3P_1$ and, to a lesser extent, with $^3F_3$; these partial waves all produce $f_2(1270)\pi$ amplitudes with $L = 1$ and 3 in the final state and differ only by Clebsch-Gordan coefficients for different helicities. In the new fit, the $^3P_1$ amplitudes shrink to quite small values, and $^3P_2$ and $^3F_3$ amplitudes grow to large values. This change is a direct consequence of the simultaneous fit to three channels of data.

We now deal with some technicalities. Small contributions due to $f_0(980)$, $f_0(1500)$ and $f_2(1565)$ are visible in mass projections of Fig. 3. The structure at $s = 2 - 2.5$ GeV^2 in the first panel (600 MeV/c) is largely due to $f_2(1565)$, not $f_0(1500)$. This contribution dies away rapidly at higher momenta. It is parametrised by the form given in Ref. [8]. Contributions from $f_0(1370)$ may be separated reliably from those due to $f_2(1270)$ but are small. The fit to $\eta\eta\pi^0$ requires contributions also from $f_0(1770)$, $f_2(1980)$ and $f_0(2105)$.

No significant physics can be extracted from these small amplitudes. If they are fitted freely to all partial waves, there is the danger that they drift to sizeable magnitudes with large destructive interferences between them. This is a well known form of instability. To avoid it, a penalty
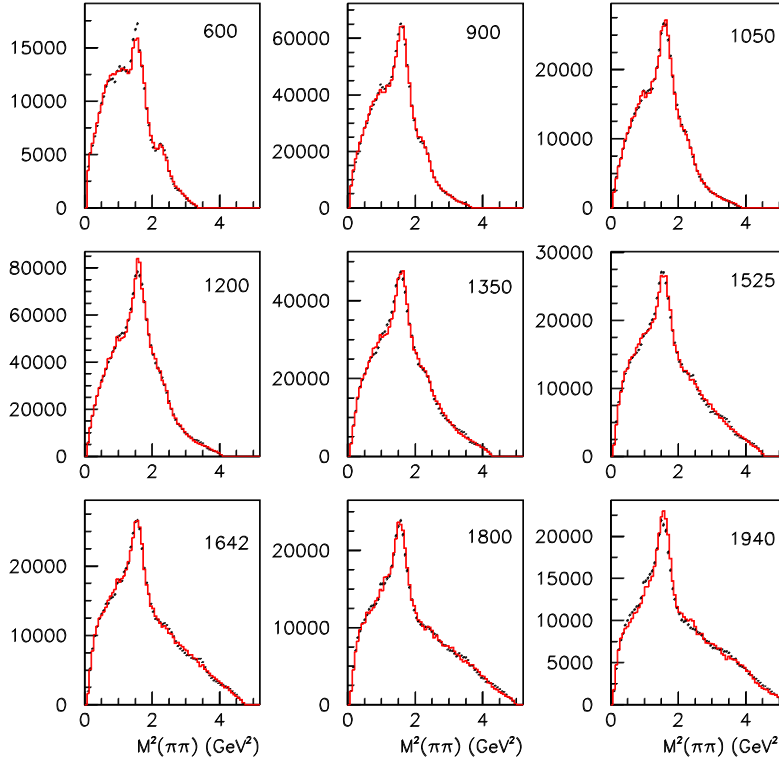
4

Figure 3: Projections on to $M^2(\eta\eta)$; histograms show the fit. Numbers in each panel indicate beam momenta in MeV/c.

function is introduced for magnitudes Λ of amplitudes. This penalty function takes the form of contributions to χ^2:

$$\chi_i^2 = [(\Lambda - \Lambda_0)/\delta\Lambda]_i^2.$$

Here Λ_0 is a target value, zero for $f_0(980)$, $f_0(1370)$, $f_2(1565)$. The denominator $\delta\Lambda$ is adjusted so that the magnitude of each partial wave contributes up to $\chi^2 = 9$ (i.e. 3σ) to the penalty function. Those amplitudes which are really needed feel little influence from the penalty function compared with very large contributions to log likelihood from individual data points; amplitudes which are not needed settle close to zero. In practice this simple procedure stabilises the small partial waves very effectively. It contributes ~ 650 to χ^2 compared with $\sim 650,000$ for log likelihood.

The $f_0(1500) \to \eta\eta$ is clearly visible in $\eta\eta\pi^0$ data and is well determined there. A first pass through the present analysis determines the branching ratio

$$BR[f_0(1500) \to \eta\eta]/BR[f_0(1500) \to \pi^0\pi^0] = 0.52 \pm 0.16. \tag{4}$$

With this branching ratio, the magnitudes of $f_0(1500)\pi$ amplitudes fitted to $3\pi^0$ agree naturally for all partial waves with those fitted to $\eta\eta\pi^0$. In the final fit, values of Λ_0 are set to magnitudes predicted from $\eta\eta\pi^0$ and equn. (4).

Contributions from $f_0(1770)$, $f_2(1980)$ and $f_0(2105)$ cannot be determined reliably from $3\pi^0$ data, because of the intrinsic systematic uncertainty in how to treat the broad background. Branching ratios for $f_0(2105)$ and $f_2(1980)$ between $\eta\eta$ and $\pi^0\pi^0$ have been determined well in Ref. [4] from a combined fit to $\bar{p}p \to \eta\eta$ and $\pi^0\pi^0$. These branching ratios are used to determine Λ_0 in the penalty functions from $\eta\eta\pi^0$ data. The branching fraction of $f_0(1770)$ to $\pi^0\pi^0$ is fitted
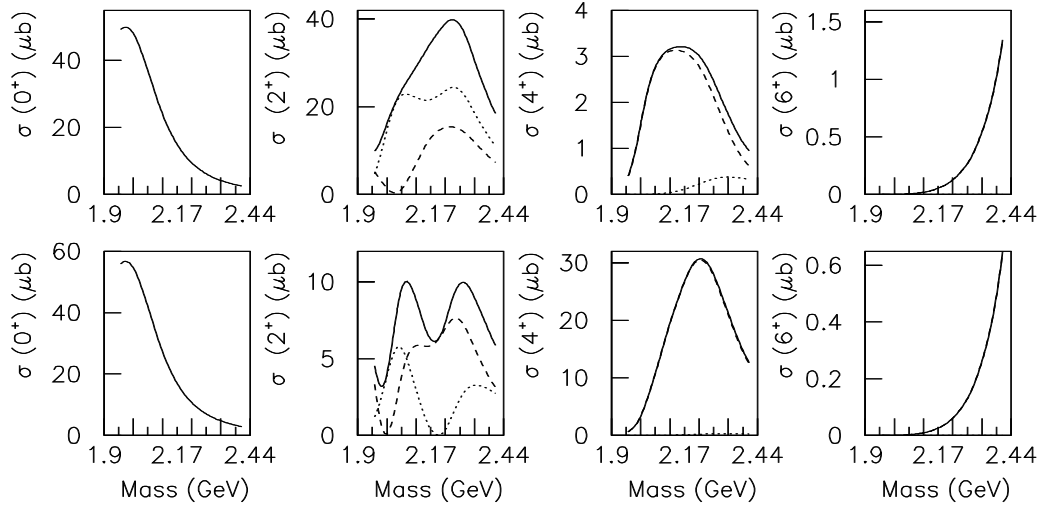
Figure 4: Intensities of 0^+, 2^+, 4^+ and 6^+ partial waves in $\bar{p}p \to \pi^0\eta$ for solution 2 (upper row) and solution 1 (lower row). Dashed curves show intensities for $^3P_2$ and $^3F_4$, dotted curves for $^3F_2$ and $^3H_4$, full curves their sum.

freely. Masses and widths of $\pi(2070)$ and $\pi(2360)$ are fixed at the more reliable values fitted to $\eta\eta\pi^0$ data; free fits to $3\pi^0$ data are consistent with those values but with larger errors of ± 60 MeV.

We begin the physics discussion with $\pi^0\eta$ and $\pi^0\eta'$. In Ref. [2], two solutions were found. That remains the case now. They are shown for $\pi^0\eta$ in Fig. 4. These solutions are quite distinct. There is no smooth transition from one solution to the other. Instead, it is necessary to change the signs of coupling constants of at least two resonances in order to jump from one solution to the other. Extensive searches of this type have not located any further solutions compatible with a simultaneous fit to $3\pi^0$. As one varies r parameters, the two previously published solutions deform continuously to those given here. The quality of the fits is indistinguishable by eye from those shown in Ref. [2]. The fit to $\pi^0\eta$ and $\pi^0\eta'$ is now better for the new solution 2: $\chi^2 = 607$ for 432 points, compared with 720 for solution 1.

The essential difference between these two solutions is that the upper of two 4^+ resonances requires $r_4 = 0.87 \pm 0.27$ for solution 2 but $r_4 = 0.30 \pm 0.31$ for solution 1. This difference is accompanied by large changes of coupling constants to $\pi^0\eta$ and $\pi^0\eta'$ for 2^+ and 4^+ states. The 4^+ intensity is much larger in solution 1 and smaller for 2^+.

In both solutions a large 0^+ amplitude is required. Much of it may be fitted as background from a pole in the region 1450–1750 MeV. However, a resonance at 2005 ± 30 MeV with $\Gamma = 300 \pm 35$ MeV is also required and gives a significant improvement in χ^2 of 290. There is further evidence for this state from $\bar{p}p \to \eta\pi^0\pi^0\pi^0$ data [9]. One expects a further 0^+ state around 2250–2360 MeV. However, adding it to either solution 1 or 2 changes χ^2 by < 73, which is not enough to establish the presence of another state. The addition of this second 0^+ state increases the errors for the lower one. In the final fit, we therefore fix the mass and width of the lower state to $M = 2025$ MeV, $\Gamma = 320$ MeV from Ref. [9].

Fits to the $3\pi^0$ data are almost identical for solutions 1 and 2 for all partial waves except 2^+, 4^+ and 6^+, and even there the main differences are for $^3H_4$ and $^3H_6$. The fit to $3\pi^0$ data again

Name	J^P	M (MeV)	Γ (MeV)	r	ΔS	$M(I=0)$ (MeV)
π_4	4^-	2250 ± 15	215 ± 25		11108	2328 ± 38
a_4	4^+	2255 ± 40	330^{+110}_{-50}	0.87 ± 0.27	2455	2283 ± 17
a_4	4^+	2005^{+25}_{-45}	180 ± 30	0.0 ± 0.2	2447	2018 ± 6
a_3	3^+	2275 ± 35	350^{+100}_{-50}		3154	2303 ± 15
a_3	3^+	2031 ± 12	150 ± 18		18410	2048 ± 8
a_2	2^+	2255 ± 20	230 ± 15	-2.13 ± 0.20	2289	2293 ± 13
a_2	2^+	2175 ± 40	310^{+90}_{-45}	-0.05 ± 0.31	1059	2240 ± 15
a_2	2^+	2030 ± 20	205 ± 30	2.65 ± 0.56	1308	2001 ± 10
π_2	2^-	2245 ± 60	320^{+100}_{-40}		2298	2267 ± 14
π_2	2^-	2005 ± 15	200 ± 40		1633	2030 ± 15
a_1	1^+	2270^{+55}_{-40}	305^{+70}_{-35}		2571	2310 ± 60
π	0^-	2360 ± 25	300^{+100}_{-50}		1955	2285 ± 20
π	0^-	2070 ± 35	310^{+100}_{-50}		1656	2010^{+35}_{-60}
a_0	0^+	(2025)	(320)		21374	2040 ± 38
a_2	2^+	1950^{+30}_{-70}	180^{+30}_{-70}	-0.05 ± 0.30	2638	1934 ± 20
π_2	2^-	(1880)	(255)		7315	1860 ± 15
a_1	1^+	1930^{+30}_{-70}	155 ± 45		2609	1971 ± 15
a_1	1^+	(1640)	(300)		232	
π	0^-	(1801)	(210)		2402	

Table 1: Masses and widths of fitted resonances for the preferred solution 2. Values in parentheses are fixed from other data. Entries in the lower half of the table are below the available mass range and may not be determined reliably. Column 6 shows changes ΔS in log likelihood when each resonance is removed from the fit to $3\pi^0$ data and all remaining parameters are re-optimised. The last column shows masses for $I = 0$, $C = +1$ resonances from Ref. [4] for comparison.

favours solution 2 by 1182 in log likelihood. We show below in Tables 1 and 2 that removing any resonance from the fit changes log likelihood S by amounts which are typically 2000. Removing any small amplitude for $f_0(980)$, $f_0(1300)$, $f_0(1500)$, etc. introduces changes in log likelihood up to 250.

Table 1 shows masses and widths of resonances in the preferred solution 2. These results supercede those of Refs. [1] and [2]. Statistical errors are very small, typically 5 MeV for masses. Errors in the Tables cover systematic variations in a large number of alternative fits (e.g. omitting $f_0(980)\pi$, $f_0(1500)\pi$ or $f_2(1565)\pi$ final states). The parameters of the 6^+ state are set to those of $a_6(2450)$ of the Particle Data Group, but there is little sensitivity to this choice. For solution 1, masses and widths of all states except 2^+ and 4^+ show changes from solution 2 no larger than statistical errors, i.e. ~ 5 MeV. Table 2 shows masses and widths for 2^+ and 4^+ states in this alternative solution.

The essential change in going from solution 2 to solution 1 is that the upper 4^+ state moves down in mass from 2255 MeV to 2220 MeV. There is a small increase in the mass of the lower 4^+ state from 2005 to 2030 MeV. What is happening is that the two 4^+ states, which have similar

Name	J^P	M	Γ	r	ΔS
		(MeV)	(MeV)		
a_4	4^+	2220 ± 20	345 ± 65	0.30 ± 0.31	2852
a_4	4^+	2035 ± 20	135 ± 45	0.0 ± 0.2	2063
a_2	2^+	2235 ± 35	200 ± 25	-1.74 ± 0.36	3658
a_2	2^+	2135 ± 45	305^{+90}_{-45}	-0.56 ± 0.53	1097

Table 2: Masses and width of resonances in the alternative solution 1. The last column shows changes ΔS in log likelihood when each resonance is removed from the fit and all remaining parameters are re-optimised.

values of r_4, are tending to merge. We have observed elsewhere that such merging of resonances of the same J^P tends to give small improvements in log likelihood through interference effects. Generally it should be regarded with suspicion.

There are two physics reasons for preferring solution 2. The first is that the upper 2^+ and 4^+ states are closer to those observed for $I = 0$, $C = +1$, shown in the final column of Table 1 for comparison. Although one state might shift significantly in mass, for example because of the opening of a nearby threshold, systematic differences of 60–105 MeV between $I = 0$ and $I = 1$ states seems unlikely. The second indication is that the fit to $I = 0$, $C = +1$ found a large positive value of r_4 for the upper resonance of 2.7 ± 0.5, closer to the present solution 1. Values of r_2 are similar for $I = 0$ and 1.

Despite differences of detail between solutions 1 and 2, the general pattern of masses and widths for $I = 0$ and $I = 1$ is similar. It is surprising that most $I = 1$ masses tend to lie 20 MeV lower than for $I = 0$. Since solution 1 tends to drag the masses of the upper 2^+ and 4^+ states down, there is the possibility that this ambiguity is everywhere having the effect of lowering masses, through correlations between partial waves. We have tried increasing all masses for $I = 1$ systematically by 20 MeV and refitting. This does not solve the problem: log likelihood increases by 820, but when masses are released, they drift down again to the solution of Table 1. The shift in mass between $I = 1$ and 0 is dictated largely by good determinations for $a_3(2031)$ and $a_2(2255)$.

Figs. 5 and 6 show intensities and phases of the dominant partial waves as a function of mass for the preferred solution 2. The figures also show intensities from fits to individual energies as squares (or triangles for $4^-[f_2\pi]_{L=5}$). In those fits, r values of 2^+ and 4^+ states are fixed at each momentum to values from the full fit. This is the origin of differences from Figs. 3 and 4 of Ref. [1]. Only magnitudes and phases of $f_2(1270)\pi$ amplitudes are set free in single-energy fits. The high partial waves are set free only at high momenta, where they are well determined. The scatter of points about the smooth curves indicates the uncertainties, mostly in phases.

We now comment on individual resonances. The low mass of the 4^- ($^1G_4$) state at 2250 MeV compared with $\rho_5(2350)$ is surprising but appears reliable. There is excellent agreement for this 4^- state with fits to $\eta\eta\pi^0$, where it also appears strongly in $a_0(980)\eta$ at 2255 ± 30 MeV with $\Gamma = 185 \pm 60$ MeV.

The 4^+ states are not accurately defined, because of the lack of polarisation information to determine values of r_4. For the lower state, r_4 is consistent with zero. At this mass, it would be surprising if $^3H_4$ made any significant contribution, because of the $\bar{p}p$ $\ell = 5$ centrifugal barrier.
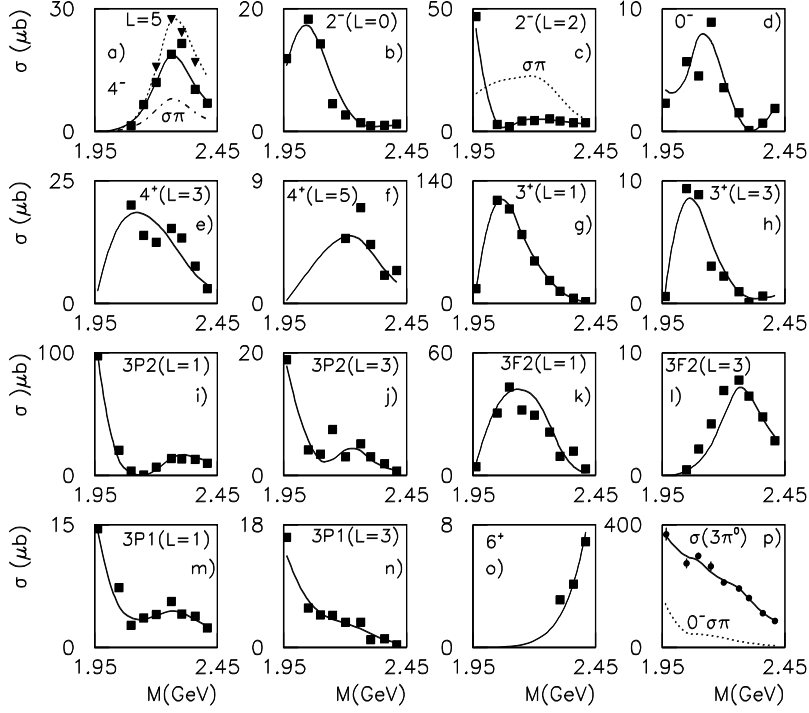
Figure 5: Intensities of individual partial waves (preferred solution 2). Squares and triangles show free fits at single energies. Full curves are for $f_2(1270)\pi$ final states. Dotted and chain curves in (a) show respectively the 4^- $f_2\pi$ amplitudes with $L = 5$ (triangles) and the $\sigma\pi$ contribution. Dotted curves in (c) and (p) show $\sigma\pi$ contributions. In (p), points and the full curve show the integrated cross section for $3\pi^0$.

The lower 3^+ state at 2031 MeV is by far the dominant partial wave at low mass. It is particularly narrow, $\Gamma = 150 \pm 18$ MeV. This narrow width is essential in order to reproduce the rapid change in angular distributions shown on Fig. 2 from 600 to 900 MeV/c. The lower 4^+ state must also be quite narrow, $\Gamma = 180 \pm 30$ MeV (like $f_4(2050)$), for the same reason. The upper 3^+ state does not appear as a peak in Fig. 5(g) because it is overwhelmed by the large amplitude from the lower resonance. It is required to explain the phase variation at high mass. There is also evidence for it from a small peak observed in the analysis of $\eta\eta\pi^0$ data [3].

Two dominantly $^3F_2$ states are required at 2255 and 2030 MeV and two dominantly $^3P_2$ states at 2175 MeV and ~ 1950 MeV. This pattern is close to that observed for $I = 0$. The strong 1950 MeV state is at the bottom of the available mass range, and its mass and width are strongly correlated. If its parameters could be determined accurately elsewhere, this would stabilise the present analysis considerably. The $a_2(2175)$ gives the smallest improvement in log likelihood, namely 1059. It may be simulated to some extent by changes to mass, width and r value of $a_2(2255)$; its contribution may also be simulated to a limited extent by a possible contribution from the missing 0^+ state in the mass range 2280–2360 MeV.

For $J^P = 2^-$, the behaviour of $L = 2$ and $L = 0$ intensities of $f_2(1270)\pi$ partial waves at low masses are interesting. There is a requirement for a very strong $L = 2$ amplitude at the lowest momentum; it is required specifically to fit the detailed structure of the mass projection of Fig. 3 at 600 MeV/c. It fits naturally to $\pi_2(1880)$, reported in an analysis of $\eta\eta\pi^0\pi^0$ data [10]. Despite the fact that this resonance is below the available mass range, omitting it changes log likelihood by a particularly large amount, 7315. A strong $2^- \to [f_2(1270)\pi]_{L=2}$ partial wave in this mass range was reported by Daum et al. [11]. Next, there is a large peak around 2030
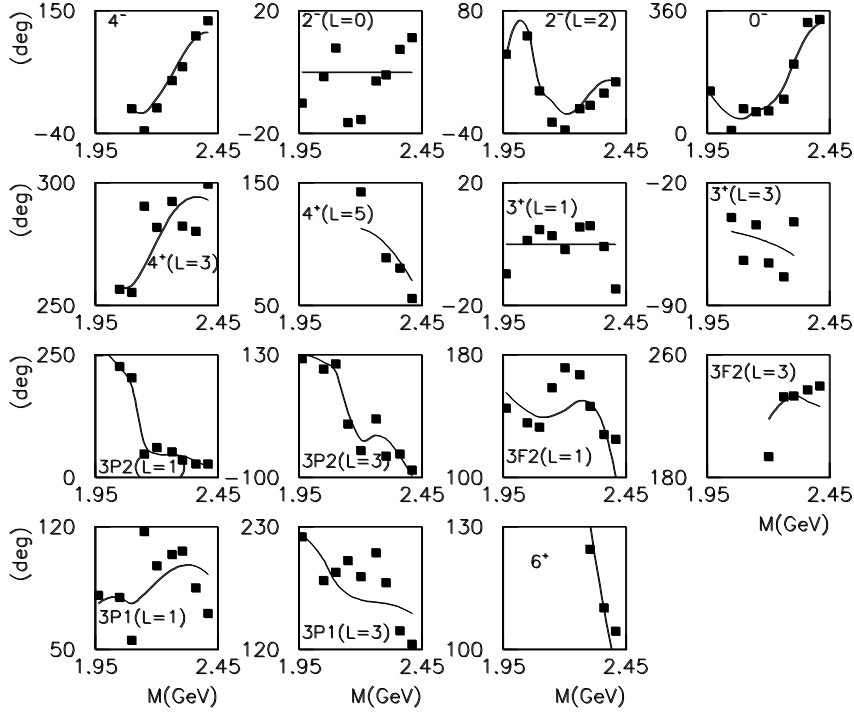
Figure 6: Phases of individual $f_2\pi$ partial waves, relative to $2^-(L = 0)$ for singlet states and relative to 3^+ for triplet partial waves.

MeV in Fig. 5(b) for $[f_2\pi]_{L=0}$. The rapid variation in these two amplitudes with $L = 0$ and 2 can be accomodated only by adding a second $\pi_2(2005)$. Without this extra state, log likelihood is worse by 1633. There is further evidence for this second π_2 in the analysis of $\eta\eta\pi^0$ data [3].

For 2^- at high masses, there is evidence for something around 2245 MeV. Without it, log likelihood is worse by 2298, a highly significant amount. However, the mass and width are poorly determined. This is because it couples weakly to $f_2\pi$, and is observed mostly in decays to $\sigma\pi$, shown by the dotted curve of Fig. 5(c). Ambiguities in the treatment of the broad σ make the systematic errors for mass and width large.

The amplitudes for $J^P = 1^+$ are the most difficult to determine, because of low multiplicity $(2J+1)$ and because of cross-talk with $^3P_2$ and $^3F_3$ decays to $f_2\pi$. There is a definite resonance at 2270 MeV, Fig. 5(m), but with sizeable errors for mass and width. The mass has decreased somewhat from that reported in the analysis of $3\pi^0$ data in Ref. [1]. In that previous analysis, a lower 1^+ state was reported at 2100 MeV. That claim is now withdrawn. The addition of the strong $a_2(1950)$ state has improved the fit by a very large amount and has reduced the $^3P_1$ amplitudes to small values peaking near threshold. Some low mass 1^+ contribution is still required, but it optimises at 1930 MeV, below the available mass range, which begins at 1960 MeV. It cannot be regarded as well defined from present data.

In summary, the mass spectrum for $I = 1$ is similar to that for $I = 0$. However, the $\pi_2(2245)$ has large errors; also $a_2(1950)$ and $a_1(1930)$ are not securely identified in mass and width, though some such contributions are definitely required. Fig. 7 shows a comparison of M^2 against radial excitation number with straight line trajectories with a slope of $1.143\,\text{GeV}^{-2}$. This is the average slope fitted to $I = 0$ states in Ref. [4]. The pion is not shown on the $^1S_0$ trajectory, because its mass is pulled strongly downwards by the instanton interaction. That may affect $\pi(1300)$ by an unknown amount. Around 1800 MeV, the VES group reports both $\pi(1800)$ and a 0^- peak in $\rho\omega$ at 1750 MeV [12]. If they are distinct, the former is a strong hybrid candidate. Fig. 7 shows
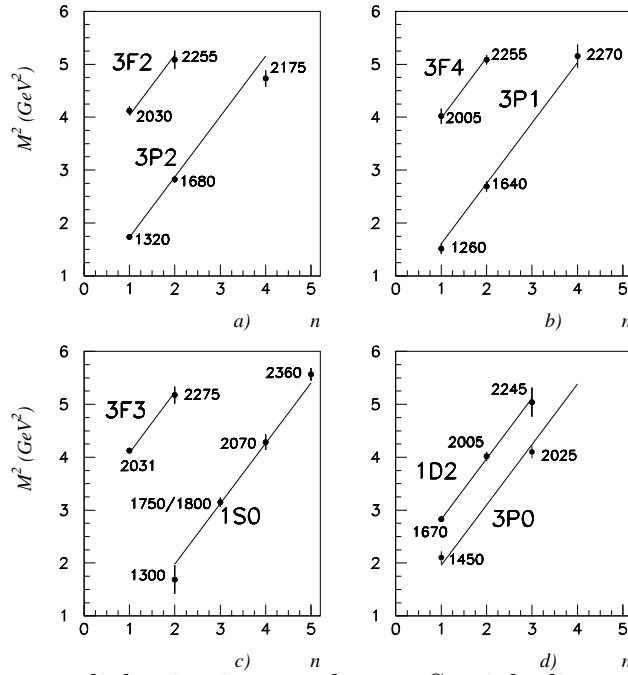
Figure 7: Plots of M^2 vs. radial exitation number n. Straight line trajectories are drawn in all cases with a slope of 1.143 GeV^{-2} from Ref. [4]. Numbers indicate masses in MeV.

the mean mass with an error covering both possibilities.

Two possible slopes 1.143 GeV^{-2} and 1.38 GeV^{-2} were discussed in Ref. [13] and trajectories of T-matrix and K-matrix poles were considered. The K-matrix poles are not discussed here, but T-matrix pole trajectories may be investigated fully. The best solution corresponds much better to the first slope. To make an explicit check, we make a set of fits restricting resonance masses to straight-line trajectories.

That for the 0^{++} sector is constructed starting from $a_0(1450)$. As discussed above, when two 0^+ resonances are introduced in the mass range 1900–2410 MeV, the 0^{++} sector becomes weakly defined and such readjustment causes only very marginal loss in log likelihood. The $^3P_2$ trajectory starts from $a_2(1320)$ with $a_2(1680)$ as the radial excitation. For a slope of 1.143 GeV^{-2}, this requires the mass of the next state to be 1980-1990 MeV, one standard deviation above $a_2(1950)$. The next state is predicted at ~ 2250 MeV. Although the mass shift required for $a_2(2175)$ is two standard deviations, we stress that this resonance gives the smallest contribution to the likelihood value. The resulting fit with slope 1.143 GeV^2 for all resonances gives log likelihood only 350 worse than the best fit. There are no visible discrepancies in fits to data and this solution may be considered acceptable under the restrictions imposed. The fit with slope 1.38 GeV^{-2} produces a solution with log likelihood worse by 2200 than the best solution. We conclude that resonance masses for the $I = 1$ $C = +1$ sector correspond approximately to the slope of 1.143 GeV^2, but not to the slope 1.38 Gev^{-2} for T-matrix poles.

1   Acknowledgement

11

References

[1] A.V. Anisovich et al., Phys. Lett. B452 (1999) 187.

[2] A.V. Anisovich et al., Phys. Lett. B452 (1999) 173.

[3] A.V. Anisovich et al., Phys. Lett. B517 (2001) 273

[4] A.V. Anisovich et al., Phys. Lett. B491 (2000) 47.

[5] Particle Data Group, Euro. Phys. J 15 (2000) 1.

[6] B.S. Zou and D.V. Bugg, Phys. Rev. D48 (1993) R3948.

[7] V.V. Anisovich et al., Phys. Rev. D50 (1994) 1972.

[8] C.A. Baker et al., Phys. Lett. B467 (1999) 147.

[9] A.V. Anisovich et al., Phys. Lett. B472 (2000) 168.

[10] A.V. Anisovich et al., Phys. Lett. B500 (2001) 222.

[11] C. Daum et al., Nucl. Phys. B182 (1981) 269.

[12] D. Amelin, Hadron Spectroscopy, in: S.-U. Chung, J.J. Willutzski (Eds.), AIP Conference Proceedings, Vol. 432 Amer. Inst. Phys., New York, (1998) p770.

[13] A.V. Anisovich, V.V. Anisovich and A.V. Sarantsev, Phys.Rev. D62 (2000) 051502, hep-ph/0003113.